Machinery Fault Diagnosis Using Advanced Correlation Filters

[1]C. K. Loo, [2]Nikos, E. Mastorakis
[1]Faculty of Engineering and Technology
Multimedia University
Melaka, Malaysia
[2]Department of Electrical Engineering and Computer Science
Hellenic Naval Academy
Piraues, GREECE

http://www1.mmu.edu.my/~ckloo
http://wseas.org/mastorakis/

Abstract: - The purpose of machine condition monitoring is to determine the present health of machineries. Capturing the abnormal symptoms of machineries from vibration signatures involves the use of signal processing algorithms on measured vibrations. However, the commonly used method such as FFT based power spectra assumes the the signal is ergodic and stationary. The FFT based method may produce unpredictable results especially in an industrial environment that subjected to random or periodic noise. Such effects can be detected, however, with second-order cyclostationary statistical method such as Degree of Cyclostationary (DCS). This paper discussed the implementation of machinery fault diagnosis using the Quad-Phase Unconstrained Optimal Tradeoff Synthetic Discriminant Function (QUOTSDF) and DCS features for fault classification. Quad-Phase Unconstrained Optimal Tradeoff Synthetic Discriminant Function (QUOTSDF) is used in this effort because of its ability to provide high discrimination while providing noise tolerance. The machine health condition is identified based on the comparison of acquired real-time vibration features with template features. The vibration data were collected from the Schenck Motor MM-61. Four machinery conditions are simulated by the motor, which are normal (no fault), bearing damage, machine imbalance, and foundation looseness. The Fast Fourier Transform (FFT) and the Degree of Cyclostationary (DCS) have been utilized for features extraction from the power spectrum of the vibration data. Fault diagnosis based on DCS features are shown to outperform FFT in accuracy.

Key-Words: - Fault diagnosis, pattern recognition, second-order cyclostationary analysis, Fast Fourier Transform, Quad-Phase Unconstrained Optimal Tradeoff Synthetic Discriminant Function, spectral analysis.

1 Introduction

Capital intensive manufacturing machineries are the heart of functionality of the manufacturing industry. In order to maximize the return of investment, it is important to ensure the adherence of machineries to planned routine, extend their useful life, eliminate break down and unplanned stoppages. To achieve these, an effective maintenance plan has to be implemented. The purpose of machine condition monitoring is to determine the present health of machineries. It is a process that captures abnormal symptoms of machineries and uses the symptoms to decide whether the machineries are associated to any faults. Since most systems operate in noisy industrial environments, some form of statistical averaging is usually required to extract reliable features. Many methods assume that the signal is ergodic and stationary such as estimating the signal variance can provide an easily computed indicator of severe faults and estimating the autocorrelation and then calculating the Fourier Transform to give signal power spectra [1]. However, these methods may produce unpredictable in an industrial environment subjected to random or periodic noise. Such effects can be detected, however, with second-order cyclostationary statistical methods such as degree of cyclostationary (DCS) [2]. Second-order cyclostationary signals are defined as those which have a periodically time-varying autocorrelation. In this paper, a comparison study of rotating machinery fault diagnosis using vibration signature based on

Fast Fourier Transform (FFT) and DCS is reported. Their practical implementation of the analysis of vibration signals of rotating machinery is discussed. The vibration signature recognition is achieved by using advanced correlation filters called the Quad-Phase Unconstrained Optimal Tradeoff Synthetic Discriminant Function (QUOTSDF) filters [3] for its ability to provide high discrimination while providing noise tolerance. Typically, QUOTSDF filter will produce sharp distinct correlation peak for patterns from the class of the filter and produce insignificant peak for patterns from other classes. The peak values are then used in deciding the class of a given pattern.

Section II of this paper describes the degree of cyclostationary. Section III describes the vibration data utilized in the fault diagnosis experiment. The features extraction methods used and QUOTDF filters are introduced in Section IV and Section 4 respectively. The structure of the fault diagnosis carried out is explained in Section V. Section VI discussed the experimental results obtained..

2 Degree of Cyclostationary

Some definitions:
Stationary: A random signal x(t) is said to be stationary at the nth-order if its time-domain nth-order moment does not depend on time t.
Cyclostationary: A random signal x(t) is said to show cyclostationarity at the nth-order if its time domain nth-order moment is a periodical function of time t.

It was mention in [4] that vibration signal display second-order cyclostationarity. Hence, we have chosen to exploit this cyclostationary property of vibration signal as another way to extract the machine condition features. The second-order cyclostationarity of a signal x(t) is also called the cyclic autocorrelation function. It gives the amount of energy in the signal that is due to cyclostationary components at cyclic frequency α, where α = 1/T and T is the cyclic period. According to [4], the cyclic autocorrelation function is defined by

$$R_x(t,\tau) = E(x(t+\tau/2)x(t-\tau/2)) = R_x(t+T,\tau) \quad (1)$$

where E indicates the mathematical expectation and τ is the lag variable. T is the cyclic period and the cyclic frequency is represented by α, where α=1/T. We have utilized the degree of cyclostationarity (DCS) for features representation. It was given by McCormick et al. in [4] as

$$DCS^{\alpha} = \frac{\sum_{\tau} \left| R_x^{\alpha}(\tau) \right|^2}{\sum_{\tau} \left| R_x^{0}(\tau) \right|^2} \quad (2)$$

or in the frequency domain

$$DCS^{\alpha} = \frac{\sum_{f} \left| S_x^{\alpha}(f) \right|^2}{\sum_{f} \left| S_x^{0}(f) \right|^2} \quad (3)$$

where S_x^{α} is the Fourier transform of R_x^{α}.

To illustrate the capability of DCS in discriminating vibration signals, let us look at Figure 1 where two DCS spectrums (DCS in frequency domain) have been plotted. Notice that there is an extra significant spike at frequency range 200-500Hz in Figure 1(b).

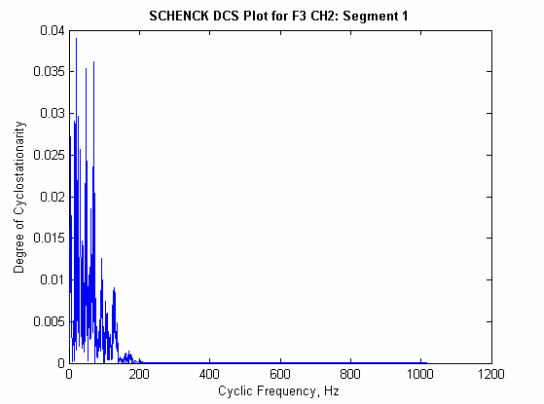

(a)

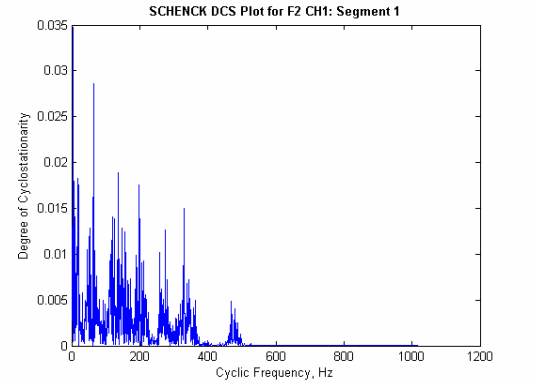

(b)

Figure 1: DCS spectrums from two different fault types.

3 Schenck Vibration Data

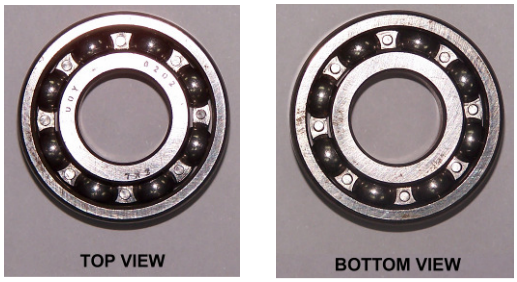

(a)

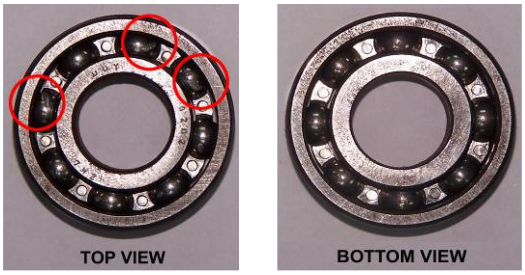

(b)

Figure 2: (a) Good bearing (b) Dented bearings

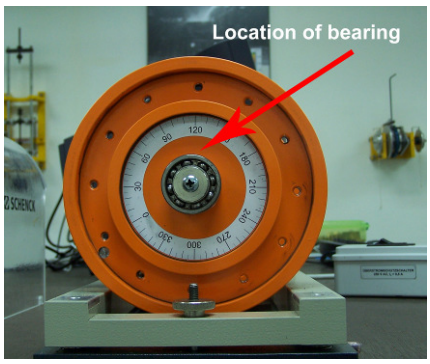

Figure 3: Location of bearing to be replaced

The vibration data that we have for this project were collected from Schenck Motor Kit MM-61 that used for the purpose of machine vibrations simulation. Four machinery conditions can be simulated by the motor kit, which are normal (no fault), bearing damage, machine imbalance, and foundation looseness. To obtain vibration data on machine running with damaged bearing, we replaced the good bearing at one end of the motor kit with a dented one. Figure 2 (a) and (b) shows the good and dented bearing respectively. Figure 3 shows the location where the bearing was replaced. To simulate imbalance, weights (screws) were added to the rotating wheel at both of the sides. The holes on rotating wheels are numbered as shown in Figure 4. In our case of simulating imbalance, we have arbitrarily added screws on number 1 to 4 for the

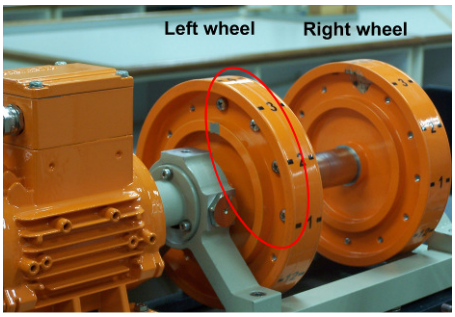

Figure 4: Weights (screws) were added to the left and right rotating wheels to simulate imbalance.

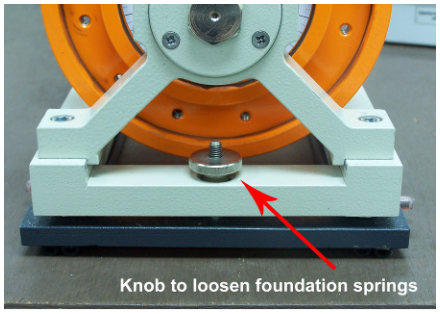

Figure 5: Location of knob on the right end.

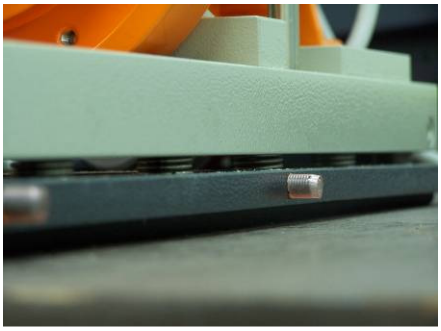

(a)

(b)

Figure 6: Difference between (a) before loosing and (b) after loosening the springs at the base of the motor kit.

left wheel and number 7 to 10 on the right wheel. There are springs mounted at the base of the motor kit. To simulate foundation looseness, we loosened the knob at both left and right ends of the motor kit (Figure 5) to reduce the springs' stiffness. The difference between before loosening and after loosening is shown in Figure 6 (a) and (b). Since more than one problem might happen at one time, we have combined them and came out with a list of eight possible conditions that might occur:

1. Normal
2. Bearing damaged
3. Imbalance
4. Loose foundation
5. Bearing damaged + Imbalance
6. Bearing damaged + Loose foundation
7. Imbalance + Loose foundation
8. Bearing damaged + Imbalance + Loose foundation

Schenck Vibration Data was collected with the aid of the several hardware and software available in the Applied Mechanics Laboratory forming a PC-based data acquisition system.

The illustration of the complete data acquisition set up is shown in Figure 7.Vibrations from motor kit MM-61 are sensed by the accelerometers MTN1100C and going through signal connector box BNC2140, signals arrive at data acquisition card PCI4552. LabVIEW® provides the interfacing between user and the data acquisition card to allow user to define how the data should be sampled and saved. An arbitrarily high sampling frequency – 102400Hz – was chosen for data collection After the sampling was done, the spectrums of the collected signals are plotted (refer to Appendix A). From the spectrums in Appendix A, we can see that the highest significant frequency component is about 35000Hz which is more than 2 times smaller than the sampling frequency. Hence, according to Shannon's sampling theorem, anti-aliasing effect should not happen here. All data were taken 30 seconds after the motor kit started to run. This was to make sure data are collected when the motor kit was running at stable condition. For each set of data, we have taken 1024000 samples which is equivalent to 10 seconds in time. Each of them is in the form of 1024000X1 matrix and saved as text (.txt) file for further manipulation.

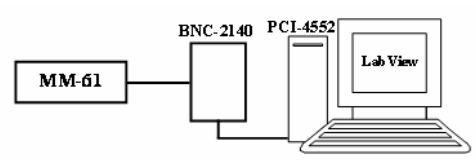

Figure 7: Illustration of data collection system

To summarize, we have taken a total number of 32 sets of data consisting of 8 machine conditions where each conditions has 4 sets of data corresponding to 4 accelerometers used.

4 Feature Extraction

Prepare Patterns with FFT Features Extraction

Starting with four matrices of size 1X1024000 which represents the data from four sensors of one machine condition, we have extracted the first 2048 samples. All the four sets of 2048 samples were multiplied by Hanning window of the same length and their FFT were taken. The magnitude square (power spectrum) of the four FFT data was calculated forming four matrices of size 1X2048. Data points from number 5 to 604 from each of the four matrices were extracted and reshaped into a matrix of size 48X50. This particular range was chosen by manual observation on the spectrums obtained and which was seen to be maximizing inter-class seperability and minimizing intra-class seperability. In our experiment, 225 patterns were prepared for each of the machine conditions. Figure 10(a) visualizes one of the patterns created using this method.

Prepare Patterns with DCS Features Extraction

The same 2048 samples extractions were done on each of the 4 rows of samples. When the first 2048 data were extracted from each of the 4 rows, their cyclic auto-correlations were calculated. The resultant output of cyclic auto-correlation (with τ=1) for each of the 2048 data samples was a 3X2048 matrix. Hence up to this point we had 4 matrices with size 3X2048. Each of them was multiplied with a 2D Hamming windows and their FFT were taken after that. Next, their spectrums for degree of cyclostationarity were obtained. After that, 600 data points were extracted starting from point number 6 to 605. This particular range was chosen by manual observation on the spectrums obtained and which was seen to be maximizing inter-class seperability and minimizing intra-class seperability. We did not start from point zero to avoid taking into account the spike in front. Again, this process was repeated for 225. For each machine condition (fault type), 100 patterns were created.

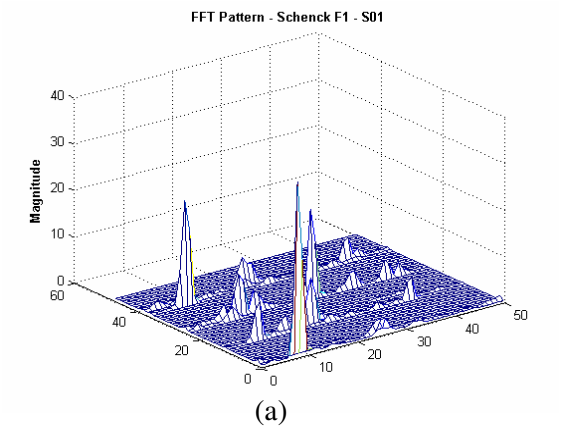

(a)

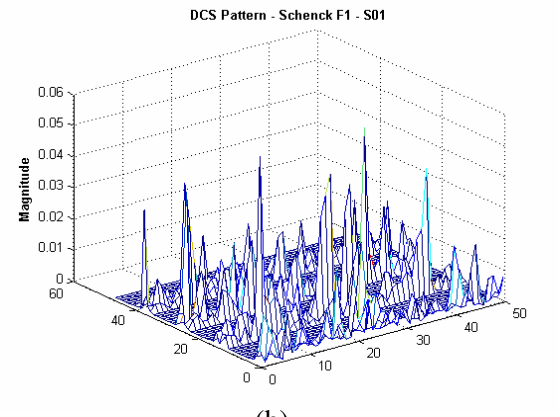

(b)

Figure 10: Visualization of a Schenck pattern created with (a) FFT features (b) DCS features.

4 QUOTSDF Filter

The basic concept of using QUOTSDF filters for classification here is to cross-correlate a template pattern with a testing pattern, producing a correlation plane. Ideally, correlation filters should suppress false class pattern, be tolerant to noise, and produce a correlation peak that be easily detected. Noise tolerance can be provided by reducing the output noise variance (ONV)[3]. On the other hand, the sidelobes can be suppressed by reducing the average correlation energy (ACE) to provide a sharp correlation peak [3]. However, minimizing the ONV and minimizing the ACE are conflicting goals. Refregier [6] first proposed a method of finding an optimal tradeoff between the two criteria and introduced the Optimal Tradeoff Synthethic Discriminant Function (UOTSDF) filter. We assume that there are N training templates, and that each template is of size $d_1 \times d_2$ containing $d = d_1 d_2$ feature values. Matrices in the frequency domain are denoted by uppercase bold characters, and vectors in the frequency domain are denoted by lowercase bold characters. Vectors in the feature domain are denoted by lowercase letters. Matrices in the feature domain are denoted by uppercase letters. Scalar elements are denoted by lowercase italicized letters. The superscript "+" refers to the conjugate transpose. The two-dimensional (2-D) FT of the i th training template is lexicographically scanned to form a column vector $\mathbf{x}_i$ containing d elements. The 2-D filter in the frequency domain is similarly scanned and represented by the column vector $\mathbf{h}$. The UOTSDF [3] filter maximizes the square of the average correlation height (ACH) defined below instead of constraining the peak values of all training templates to a specified value, and the resulting filter becomes simpler to compute.

$$ACH = \left| \frac{1}{N} \sum_{i=1}^{N} \mathbf{h}^{+} \mathbf{x}_i \right| = \left| \mathbf{h}^{+} \mathbf{m} \right| \tag{4}$$

Where $\mathbf{m}$ is the average of the N vectors $\mathbf{x}_1, \mathbf{x}_2, \ldots, \mathbf{x}_N$. Maximizing the square of ACH leads to the UOTSDF filter given below [3],

$$\mathbf{h} = \left(\alpha \mathbf{D} + \sqrt{1-\alpha} \mathbf{C} \right)^{-1} \mathbf{m} \tag{5}$$

where $\mathbf{C}$ is a $d \times d$ diagonal matrix containing the elements of the input noise power spectral density along its diagonal and $\mathbf{D}$ is a $d \times d$ diagonal matrix containing the average power spectrum of the training templates placed along its diagonal. α is the relative weight for noise tolerance and peak sharpness. If the testing pattern is similar to the template pattern, or in other words they belong to the same class, the correlation output will have a large peak value. On the other hand, if they are coming from different classes, the peak value would not be significant. From the foregoing research [3], it may beneficial to quantize the phase of input template Fourier Transform and the filter $\mathbf{h}$ to four phase values. It was found that the correlation peaks were further sharpened and the memory storage requirement of filters is reduced. Hence the resulting filter will be named QUOTSDF filter where each element in the filter array will take on ± 1 for the real component and $\pm j$ for the imaginary component in the following manner.

In Schenck vibration monitoring experiment, eight independent QUOTSDF filters were created to represent the eight different motor health conditions.

Template patterns are created according to Equation (5) by utilizing 60 training patterns from each of the machine conditions.

$$\mathbf{h}_{\mathrm{QUOTSDF}} = \begin{cases} +1 & \mathrm{Re}\,al(\mathbf{h}) \geq 0 \\ -1 & \mathrm{Re}\,al(\mathbf{h}) < 0 \\ +j & \mathrm{Im}(\mathbf{h}) \geq 0 \\ -j & \mathrm{Im}(\mathbf{h}) < 0 \end{cases} \quad (6)$$

5 Fault Diagnosis

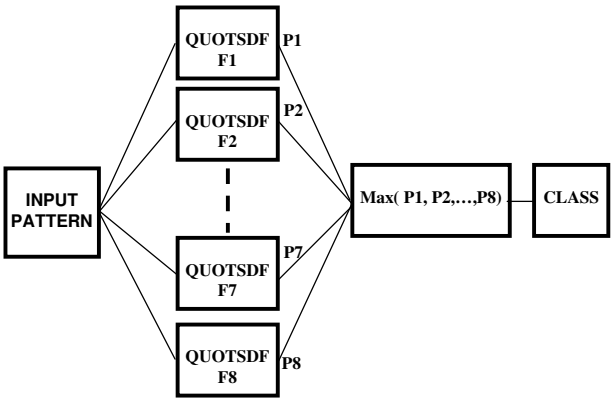

Figure 11: Structure of decision making network.

As shown in Figure 11, eight QUOTSDF filters have been used. Each of the filters was created with 60 training patterns from their respective fault class. While classifying an input pattern, the pattern was fed into each of the templates available in the network and cross-correlation was performed. The peak values from the outputs of the cross-correlation`s (P1 to P8 in this case) were taken to check for the highest value. The class of the QUOTSDF filter which produced the highest peak value was taken as the class of belonging of the input pattern. This was done to all the other torque levels except the number of QUOTSDF filters within their decision making network was different, depending on the available data sets.

A pattern (training or input) was prepared by taking 1024 data points from each of the 8 sensors in the same time period. Cyclic autocorrelation for each of the 8 sets of 1024 data points were obtained. Then, they were multiplied by a Hamming window before their fast Fourier transform (FFT) was taken. After that, data points contained in the frequency range of 5Hz to 55Hz (approximately 300 data points) were extracted, forming 8 sets of 300 points data. It was then reshaped into a matrix of size 48X50.

6 Experimental Results

Table 1: Classification Results for Schenck Patterns Using FFT in Features Extraction

Class #	%Correct	%Wrong	%Undecided
1	96.89	3.11	0.00
2	63.56	36.44	0.00
3	98.67	1.33	0.00
4	84.89	15.11	0.00
5	68.89	31.11	0.00
6	81.33	18.67	0.00
7	96.44	3.56	0.00
8	66.67	32.89	0.44
Overall	82.17	17.39	0.44

Table 2: Classification Results for Westland Patterns Using DCS in Features Extraction

Class #	%Correct	%Wrong	%Undecided
1	100.00	0.00	0.00
2	62.67	37.33	0.00
3	96.44	3.56	0.00
4	98.67	1.33	0.00
5	79.11	20.89	0.00
6	87.11	12.89	0.00
7	100.00	0.00	0.00
8	88.44	27.00	0.00
Overall	89.06	10.94	0.00

In this experiment, 225 unseen data for each fault class represents the test set. The classification results for Schenck patterns using FFT features and DCS features are shown in Table 1 and Table 2. The QUOTSDF filter is very successful in detecting a single motor fault mode such as imbalance and

loose foundation. It is relatively poor in identifying single bearing fault than other fault modes. However, the fault diagnosis accuracy is improved in case 6 (multiple faults) despite the presence of the bearing fault. It is evident from Table 4 that fault diagnosis based on DCS features outperforms FFT features. This experiment ended up with an overall of 89.06% correct classification for DCS features and 82.17% for FFT features. The overall resulting classification by QUOTSDF filters of different faults occurring in the Schenck motor, proved to be reasonable good. The QUOTSDF filters are able to detect and distinguish each fault successfully. It also successfully differentiated between single and multiple faults when presented with the test set. This classification of single and multiple faults achieved by the QUOTSDF filters is not possible by utilizing the features of the DCS features by means of visual inspection. The results of the present work showed that DCS feature extraction is a powerful tool in preprocessing raw measured vibration data. It is also evident that a selected set of the extracted features could be used an input vector to QUOTSDF filters to detect and identify the exact type of fault occurring in the rotating machinery. Although no direct comparison to other classification methods are made here, QUOTSDF filter is attractive for its simplicity and optimal class differentiability. Moreover, the preprocessing approach taken in this study is to work on the whole signal rather than the changes on the amplitude of a specific frequency range. Preprocessing the whole signal enables detection of any fault feature which occurs across the whole range of frequency. This method has a great advantage if an intelligent system is built for on-line condition monitoring and fault diagnosis of rotating machinery. This intelligent system may detect and identify other dominant fault features by considering the whole vibration signal rather any specific frequency range.

Table 4 Summarized Overall Percentage of Correct Classification

FFT	DCS
82.17%	89.06%

7 Conclusion

The basic theory of the classification methodology and the capability of using QUOTSDF filters to perform machinery faults diagnosis have been reviewed by using DCS and FFT spectrum to represent the features. The fault diagnosis was done by a simple voting scheme using the peak values from the correlation output. The results presented and discussed in this work show that DCS transform were utilized successfully to preprocess seven different types of vibration signals obtained a Schench motor drive-line. Then the QUOTSDF filter are used on the preprocessed data in order to determine its health condition by classifying different kinds of fault and differentiate between single and multiple faults. From the investigation carried out the following points can be concluded: the combination of DCS features with the QUOTSDF filters provided a useful tool for intelligent diagnostics of faults in rotating machinery and diagnostics of faults based on DCS outperforms FFT for its ability to extract useful information from signal that exhibits periodically time-varying autocorrelation. However, using DCS and FFT were found to be relatively poorer in detecting bearing faults in comparison to the other faults investigated. The reasons for poor performance of bearing fault detection will be subjected to future investigation.

References:

[1] W. R. Charles, Vibration – Machine & Systems Condition Monitoring Series, Coxmoor Publishing Company, 1998.

[2] W. A. Gardner, "Exploitation of spectral redundancy in cyclostationary signals," IEEE Signal Processing Magazine, vol. 8, no. 2, pp. 14-36, 1991.

[3] B. Vijayakumar, "Reduced Complexity Correlation Filters," US2005/0018925A1, United States Patent Application Publication, 2005.

[4] A.C. McCormick, and A. K. Nandi, "Cyclostationarity in rotating machine vibrations," Meachanical Systems and Signal Processing, vol. 12, no. 2, pp. 225-242, 1998.

[5] C. Capdessus, M. Sidahmed, and J. L. Lacoume, "Cyclostationary process: application in gear faults early diagnosis," Mechanical Systems and Signal Processing, vol. 14, no. 3, pp. 371-385, 2000.